

H3F3A K27M mutations in thalamic gliomas from young adult patients

Koki Aihara, Akitake Mukasa, Kengo Gotoh, Kuniaki Saito, Genta Nagae, Shingo Tsuji, Kenji Tatsuno, Shogo Yamamoto, Shunsaku Takayanagi*, Yoshitaka Narita, Soichiro Shibui, Hiroyuki Aburatani and Nobuhito Saito

Department of Neurosurgery, Graduate School and Faculty of Medicine, The University of Tokyo, Tokyo, Japan (K.A., A.M., K.S., S.T.*, N.S.); Genome Science Division, Research Center for Advanced Science and Technology, The University of Tokyo, Tokyo, Japan (K.A., K.G., G.N., S.T., K.T., S.Y., H.A.); Department of Neurosurgery and Neuro-Oncology, National Cancer Center Hospital, Tokyo, Japan (Y.N., S.S.)

Corresponding authors: Akitake Mukasa, MD, PhD, Department of Neurosurgery, The University of Tokyo Hospital, 7-3-1 Hongo, Bunkyo-ku, Tokyo 113-8655, Japan (mukasa-nsu@umin.ac.jp); Hiroyuki Aburatani, MD, PhD, Genome Science Division, Research Center for Advanced Science and Technology (RCAST), The University of Tokyo, 4-6-1 Komaba, Meguro-ku, Tokyo 153-8904, Japan (haburata-tyk@umin.ac.jp).

Introduction. Mutations in *H3F3A*, which encodes histone H3.3, commonly occur in pediatric glioblastoma. Additionally, *H3F3A* K27M substitutions occur in gliomas that arise at midline locations (eg, pons, thalamus, spine); moreover, this substitution occurs mainly in tumors in children and adolescents. Here, we sought to determine the association between *H3F3A* mutations and adult thalamic glioma.

Methods. Genomic *H3F3A* was sequenced from 20 separate thalamic gliomas. Additionally, for 14 of the 20 gliomas, 639 genes—including cancer-related genes and chromatin-modifier genes—were sequenced, and the Infinium HumanMethylation450K BeadChip was used to examine DNA methylation across the genome.

Results. Of the 20 tumors, 18 were high-grade thalamic gliomas, and of these 18, 11 were from patients under 50 years of age (median age, 38 y; range, 17–46), and 7 were from patients over 50 years of age. The *H3F3A* K27M mutation was present in 10 of the 11 (91%) younger patients and absent from all 7 older patients. Additionally, *H3F3A* K27M was not detected in the 2 diffuse astrocytomas. Further sequencing revealed recurrent mutations in *TP53*, *ATRX*, *NF1*, and *EGFR*. Gliomas with *H3F3A* K27M from pediatric or young adult patients had similar, characteristic DNA methylation profiles. In contrast, thalamic gliomas with wild-type *H3F3A* had DNA methylation profiles similar to those of hemispheric glioblastomas.

Conclusion. We found that high-grade thalamic gliomas from young adults, like those from children and adolescents, frequently had *H3F3A* K27M.

Keywords: thalamic glioma, young adult, *H3F3A* mutation.

Gliomas of the thalamic region are relatively rare and constitute ~1% of all brain tumors.^{1–3} Thalamic gliomas are generally difficult to treat because the tumors are located deep within the brain and, therefore, are rarely amenable to radical surgical resection.⁴ Thus, development of a novel anticancer drug is needed to treat these tumors. Schwartzentruber et al⁵ recently reported that more than 30% of pediatric glioblastoma multiforme (GBM) tumors carry a mutation in the *H3F3A* gene, which encodes the replication-independent histone 3 variant H3.3. There are 2 common mutations (K27M and G34R/V) in human *H3F3A* that each result in an amino acid substitution within the histone tail. In a study of 784 glioma samples of all grades and histological diagnoses and from patients of all ages, the *H3F3A* K27M mutation was highly specific to GBM and was found mainly in younger patients (median age, 11 y; range, 5–29), including several patients with

thalamic GBM. Wu et al⁶ also reported a high frequency of *H3F3A* mutations in pediatric gliomas and that 78% of diffuse intrinsic pontine gliomas (DIPGs) and 22% of nonbrainstem pediatric GBM carry a mutation in *H3F3A* or in a related gene, *HIST1H3B*, which encodes the histone H3.1; each of these mutations causes a K27M amino acid substitution in the respective protein. Sturm et al⁷ further showed that these mutant tumors have distinct methylation profiles and that the *H3F3A* K27M mutation most often occurs in tumors located in the midline of the brain, such as in the thalamus, brainstem, or spine. In contrast, G34R/V mutations were found in hemispheric gliomas. Although 71%–78% of DIPGs are known to have a K27M mutation,^{6,8} to our knowledge no study has focused on the *H3F3A* K27M mutation in thalamic gliomas. Here, we analyzed the prevalence and significance of the K27M mutation, especially for adult patients with thalamic glioma.

Received 16 May 2013; accepted 4 August 2013

© The Author(s) 2013. Published by Oxford University Press on behalf of the Society for Neuro-Oncology. All rights reserved.
For permissions, please e-mail: journals.permissions@oup.com.

Materials and Methods

Patients and Samples

From April 1997 to March 2013, 27 adult patients (>16 y of age) with primary thalamic glioma were treated at Tokyo University Hospital or the National Cancer Center Hospital (Table 1). Histological diagnoses were made by a senior neuropathologist from the respective treatment centers and according to World Health Organization guidelines. There were 15 GBM, 9 anaplastic astrocytomas (AAs), and 3 diffuse astrocytomas (DAs). Of the 3 low-grade gliomas, 2 were located bilaterally; in contrast, most high-grade gliomas were not bilateral (left, 12; right, 11; bilateral, 1). We were able to obtain samples of freshly frozen tumor tissue for 16 of the 27 cases; and for 14 of these 16 cases, paired, normal blood samples were available; moreover, formalin-fixed, paraffin-embedded samples of tumor tissue were available for 4 of the other 11 cases. In all, tissue samples were available for 20 of the 27 cases. The study was approved by the ethics committees of the University of Tokyo Hospital and the National Cancer Center Hospital. Each patient provided written informed consent.

DNA Extraction

The AllPrep DNA/RNA Micro kit (Qiagen) was used according to the manufacturer's instructions to extract genomic DNA from freshly frozen tumor tissue. Formalin-fixed, paraffin-embedded samples were deparaffinized with xylene, and a QIAamp DNA Mini kit (Qiagen) was then used to extract genomic DNA from these tumor samples. For the 14 cases for which tumor tissues and a paired, normal blood sample were available, a DNA extraction kit (Qiagen) was used to extract control genomic DNA from the paired blood sample.

Sanger Sequencing

For the 20 cases in which DNA from tumor tissue was available, the Sanger method was used to sequence the DNA. Oligo primers were designed to amplify a target region within *H3F3A* (sense 5'- TCAATGCTGGTAGGTAAGTAAGGA -3', antisense 5'- GGTTTCTTACCCTCCAGT -3'; product size: 152 bp). The high-fidelity DNA polymerase KOD-plus (Toyobo) and optimized thermal conditions were used to perform PCR, and the PCR products

Table 1. Patient characteristics and *H3F3A* status

Sample ID	Age	Location	OS (mo)	Surgery	Treatment	<i>H3F3A</i>	MGMT Promoter
GBM1 ^{a,b}	17	Right	8.9	PR	RT + TMZ	K27M	u
AA1	19	Bilateral	30.6	Biopsy	RT + ACNU	-	-
AA2 ^{a,b}	20	Left	9.9	Biopsy	RT + TMZ	K27M	u
GBM2 ^{a,b}	27	Multiple ^d	3.8	PR	RT + TMZ	K27M	u
GBM3 ^{a,b}	34	Right	12.6	STR	RT + ACNU	K27M	u
AA3	37	Right	26.1	Biopsy	RT + TMZ	K27M	-
GBM4 ^{a,b}	38	Left	9.8	Biopsy	RT + TMZ	K27M	u
AA4	38	Left	17.7	Biopsy	RT + ACNU	WT	-
GBM5 ^{a,b}	39	Right	10.4	PR	RT + TMZ	K27M	u
AA5 ^b	41	Left	20.6	PR	RT + TMZ	K27M	u
AA6 ^{a,b}	43	Left	15.6	Biopsy	RT + TMZ	K27M	m
GBM6	45	Left	30.8	Biopsy	RT + ACNU	-	-
GBM7 ^{a,b}	46	Right	1.6 ^f	GTR	RT + TMZ	K27M	u
AA7	47	Right	24.3	Biopsy	RT + ACNU	-	-
GBM8	48	Left	65.8	Biopsy	RT + TMZ	-	-
GBM9 ^b	50	Right	3.9	Biopsy	RT + TMZ	WT	u
GBM10	53	Left	7.3	Biopsy	RT + TMZ	-	-
AA8 ^{a,b,c}	57	Multiple ^e	110.2 ^f	Biopsy	RT + ACNU	WT	m
GBM11 ^{a,b,c}	62	Left	19.4	Biopsy	RT + TMZ	WT	u
GBM12 ^{a,b}	64	Left	30.4	STR	RT + TMZ	WT	m
GBM13 ^a	71	Left	3.5	Biopsy	RT + TMZ	WT	-
GBM14	73	Left	17.9	Biopsy	RT + TMZ	-	-
GBM15 ^{a,b}	73	Right	0.7	Biopsy	RT + TMZ	WT	u
AA9	78	Right	0.3	Biopsy	No therapy	WT	-
DA1	28	Bilateral	21.1	Biopsy		-	-
DA2 ^a	29	Bilateral	9.2 ^f	Biopsy		WT	-
DA3	30	Left	124.4 ^f	Biopsy		WT	-

Abbreviations: OS, overall survival; GTR, gross total resection; STR, subtotal resection; PR, partial resection; RT, radiotherapy; TMZ, temozolomide; ACNU, nimustine hydrochloride; WT, wild-type; m, methylated; u, unmethylated; -, not available.

^aSpecimen subjected to targeted sequence analysis.

^bSpecimen subjected to global methylation profile analysis.

^cSpecimen of recurrence.

^dRight thalamus, left temporal lobe, and fourth ventricle.

^eRight thalamus, left cerebellopontine angle, cerebellum surface, and fourth ventricle.

^fStill alive at last follow-up.

were then evaluated on a 2% agarose gel and subsequently purified. The Big Dye Terminator kit (Applied Biosystems) was used for each sequencing reaction; both strands of each PCR product were sequenced, and each sample was analyzed on an ABI 3130xl capillary sequencer (Applied Biosystems).

Targeted Sequencing

For the 14 cases for which a tumor sample and a paired, normal blood sample were available, we used the Haloplex system (Agilent) to amplify and analyze the sequences of 639 selected genes (see Supplementary Table S1). These selected genes included *H3F3A*, *HIST1H3B*, genes often mutated in gliomas (such as *IDH1/2*, *ATRX*, *TP53*, *NF1*, *EGFR*, *PDGFRA*), other frequently mutated cancer genes, and chromatin-modifier genes. Target regions were enriched using Haloplex technology following the manufacturer's protocols. A HiSeq2500 system (Illumina) set in rapid mode was used to sequence the amplified targets as 150-bp paired-end reads. The median coverage was 348-fold, and more than 93% of target regions were covered by at least 10 reads (see Supplementary Table S2). The Burrows–Wheeler Aligner algorithm v0.5.9⁹ was used to map this sequence data onto the reference genome (hg19), and somatic mutations were identified with the Genome Analysis Toolkit Unified Genotyper v1.6.13.¹⁰ The tumor-specific mutations were identified by comparing results from tumor DNA and blood DNA and were annotated with Annovar (23 October 2012).¹¹ Finally, we used the Integrative Genomics Viewer v2.2¹² to check these mutations, and we excluded artifact mutations.

Methylation-specific PCR

The EZ DNA Methylation kit (Zymo Research) was used according to the manufacturer's protocol to conduct bisulfite reactions with each genomic DNA sample (250 ng). DNA methylation status of the O⁶-methylguanine methyltransferase (*MGMT*) promoter was then determined by methylation-specific PCR as described by Esteller et al.¹³

Global Analysis of DNA Methylation

The Infinium HumanMethylation450 BeadChip (Illumina) was used according to the manufacturer's instructions to examine the genome-wide DNA methylation profiles of 14 high-grade thalamic gliomas. Previously published⁷ methylation data from additional glioblastoma samples ($n = 136$) and from control samples ($n = 6$; 2 adult normal brain and 4 fetal normal brain) were obtained from the National Center for Biotechnology Information's Gene Expression Omnibus (<http://www.ncbi.nlm.nih.gov/geo>). The following filtering steps were used to select probes for unsupervised clustering analysis. Probes targeting the X and Y chromosomes and probes containing a single nucleotide polymorphism (dbSNP130 common) within 5 base pairs of and including the targeted cytosine–phosphate–guanine (CpG) site were removed. The standard deviation of β -values for each probe was calculated, and the top 8000 probes were selected.

Statistical Analysis

Overall survival was analyzed using the Cox regression analysis or the Kaplan–Meier method, and the log-rank test was used to make universal assessments of Kaplan–Meier plots. The frequency of methylation of the *MGMT* promoter and of other genes was analyzed by Fisher's exact test, and Welch's *t*-test was used to compare the average age of the *H3F3A* K27M group with that of the wild-type *H3F3A* group. $P < .05$ was considered significant. Statistical calculations were carried out using R v2.15.2 (<http://www.cran.r-project.org>).

Results

Frequency and Characteristics of Patients Harboring the *H3F3A* K27M Mutation

Among the 18 high-grade thalamic gliomas that we subjected to sequence analysis, 10 (56%) tumors had an *H3F3A* K27M mutation, while none of the 18 tumors harbored an *H3F3A* mutation at G34. Remarkably, 10 (91%) of the 11 tumors that were from patients under 50 years of age (median age, 38 y; range, 17–46) had the *H3F3A* K27M mutation; in contrast, the *H3F3A* K27M mutation was not found in any of the 7 tumors that were from patients over 50 years of age (Table 1). The patients with the *H3F3A* K27M mutation were significantly younger than those with wild-type *H3F3A* alleles (34.2 vs 61.6 y; $P = .0003$). The *H3F3A* K27M mutation was not detected in DAs from patients who were 29 or 30 years of age.

Targeted Sequence Analyses for Selected Genes

Among the 14 cases that were subject to targeted sequence analysis, tumor DNA samples from cases GBM4 and GBM11 each had mutations in mismatch repair genes and had a higher than average number of mutations; the average number of nonsynonymous mutations in DNA samples from all tumors except these 2 GBM specimens was 3.83 (0–8) (see Supplementary Table S3), while the numbers of nonsynonymous mutations in the DNA samples from GBM4 and GBM11 were 32 and 165, respectively. GBM4 had a mutation in the mismatch repair gene *MSH2* (MutS homolog 2). In the case of GBM11, which recurred after treatment with the alkylating agent temozolomide, mutations were identified in 2 mismatch repair genes, *PMS2* (postmeiotic segregation increased 2) and *MLH3* (MutL homolog 3); moreover, 158 (96%) of 165 mutations found in this tumor were G/C to A/T transitions. Therefore, GBM11 apparently had a hypermutator phenotype.¹⁴ Because most of the mutations in these 2 cases (GBM4 and GBM11) could have accumulated passively owing to the lack of mismatch repair function, we excluded the mutation data from these cases for the subsequent analyses.

Consistent with previously reported data,⁵ *H3F3A*-mutant high-grade gliomas frequently also had mutations in *TP53*, *ATRX* (2/7 [28.6%] of *H3F3A* K27M-mutant tumors vs 0/4 [0%] of wild-type *H3F3A* tumors; $P = .49$), and *NF1* (3/7 [42.9%] vs 0/4 [0%]; $P = .24$) (Fig. 1). In contrast, wild-type *H3F3A* tumors had *EGFR* mutations more frequently than did *H3F3A* K27M-mutant tumors (0/7 [0%] vs 2/4 [50%]; $P = .11$). There were no recurrent mutations other than *H3F3A*, *TP53*, *ATRX*, *NF1*, and *EGFR*. Wu et al⁶ reported that 18% of DIPGs had a *HIST1H3B* K27M mutation, but we did not find *HIST1H3B* mutations in any of the 14 tissue samples evaluated, even in samples from wild-type *H3F3A* tumors. Additionally, none of the 14 tumors examined had an *IDH1* or an *IDH2* mutation.

Recently, Fontebasso et al¹⁵ found that mutations in the *SETD2* gene, which encodes an H3K36 trimethyltransferase, occurred in 15% of hemispheric pediatric GBMs, and mutations in *SETD2* and *H3F3A* were mutually exclusive. Based on these findings, we also sequenced genes that potentially affect histone modification, such as the H3K27 methyltransferase *EZH2*, the H3K27 demethylase *KDM6A*, the H3K27 acetyltransferase *EP300*, and *CREBBP*. We identified a *KDM6A* mutation (p.R1213L), located in

	GBM1	AA2	GBM2	GBM3	GBM5	AA6	GBM7	AA8	GBM12	GBM13	GBM15	DA2
H3F3A												
TP53												
ATRX												
NF1												
EGFR												
PDGFRA												
IDH1/2												
ARID1B												
ATM												
BCOR												
BIRC2												
BTK												
BUB1B												
CHD8												
CREBBP												
DNAH8												
FGFR1												
GNAS												
IGF2R												
KDM6A												
KDR												
MLL3												
MYH9												
PHC2												
PIK3R1												
PRPF4B												
SMC3												
SPGE												
THBS1												
TNKS												
USP9X												
WNK2												

Fig. 1. Nonsynonymous mutations identified via targeted sequencing. Each row represents a specific gene, and each column represents one sample. The shaded boxes represent identified nonsynonymous mutations.

the JmjC domain, in one case of DA with wild-type *H3F3A* and a *CREBBP* mutation in one case of GBM with the *H3F3A* K27M mutation. However, we did not find mutations in any of these genes in any of the 4 analyzed cases of high-grade glioma that lacked an *H3F3A* K27M mutation.

In addition, we found an *FGFR1* mutation (N546K) in one GBM (GBM5) with *H3F3A* K27M. Schwartzenuber et al⁵ also reported an *FGFR1* mutation (K656E) in an *H3F3A* K27M-mutant tumor.³ Both of these *FGFR1* mutations reportedly enhance kinase activity.¹⁵

Methylation Status of the MGMT Promoter

We analyzed methylation at the *MGMT* promoter in samples from 14 adults with high-grade gliomas whose DNA was suitable for such analysis; the *MGMT* promoter in 11 (79%) of these tumors was unmethylated. In particular, the *MGMT* promoter was frequently unmethylated in samples of thalamic glioma with an *H3F3A* K27M mutation from young adults (8/9; 89%). The rate of unmethylated *MGMT* promoter was higher in the group of samples analyzed in this study than in a group of high-grade gliomas from all locations that we analyzed previously (43/75; 57%),¹⁶ but the difference between these rates was not statistically significant ($P = .23$).

Global DNA Methylation Profiles of Thalamic Gliomas

The genome-wide Infinium methylation data demonstrated that adult thalamic high-grade gliomas with the *H3F3A* K27M mutation

had methylation profiles distinct from those of adult thalamic high-grade gliomas that lacked the *H3F3A* K27M mutation (Fig. 2). In the hierarchical clustering analysis that included methylation profile data from previously categorized pediatric and adult gliomas,⁷ the adult thalamic high-grade gliomas harboring the *H3F3A* K27M mutation clustered within the same “K27” category as did the pediatric gliomas harboring *H3F3A* K27M. In contrast, adult thalamic high-grade gliomas with wild-type *H3F3A*, which had a variety of methylation profiles, did not cluster into the K27 category, but clustered within several other categories, including “mesenchymal” and “classic.” One recurrent anaplastic astrocytoma (AA8) that was wild-type for *H3F3A* had a profile that was similar to those of the tumors in the K27 category, but this profile seemed to be located outside the cluster in the K27 category.

Prognostic Value of the H3F3A K27M Mutation

For the 16 cases for which a primary tumor sample was analyzed, the median overall survival of patients with GBM and those with AA was 8.9 months and 15.6 months, respectively. The median overall survival of patients with high-grade gliomas (GBM or AA) was 9.9 months, and progression-free survival of these patients was 5.3 months. In these cases of high-grade glioma, the median overall survival of patients with *H3F3A* K27M-mutant tumors was 10.4 months (GBM, 9.8 mo; AA, 15.6 mo) and that of patients with wild-type *H3F3A* tumors was 3.5 months (GBM, 3.5 mo; AA, 0.3 mo). There was no statistical difference in overall survival ($P = .80$) or progression-free survival (6.0 vs 1.8; $P = .44$) between these 2 groups (Fig. 3).

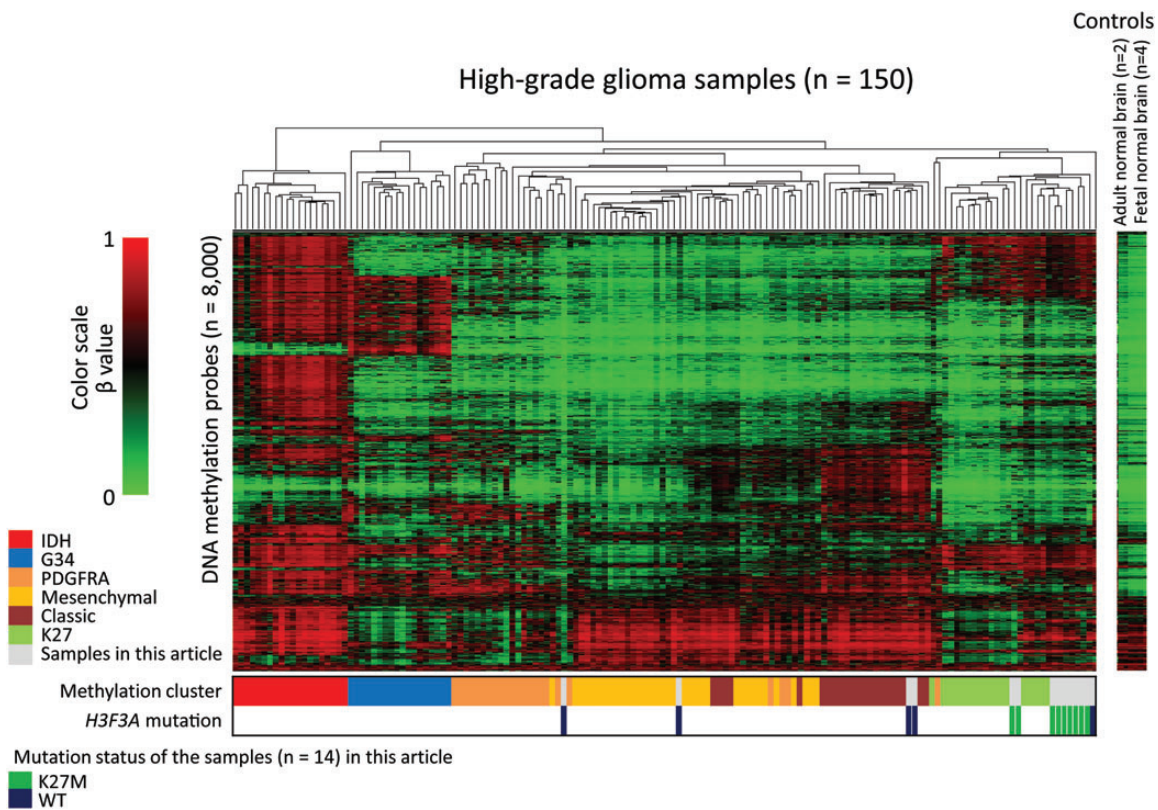


Fig. 2. Heatmap of methylation levels (β -value) in 150 high-grade gliomas, including 14 thalamic gliomas analyzed in this study. Supervised clustering was performed using 8000 selected Infinium probes. Each row represents a probe, each column represents one sample. For each sample, annotation of methylation cluster and *H3F3A* mutation status are indicated by colored boxes at the bottom of the map.

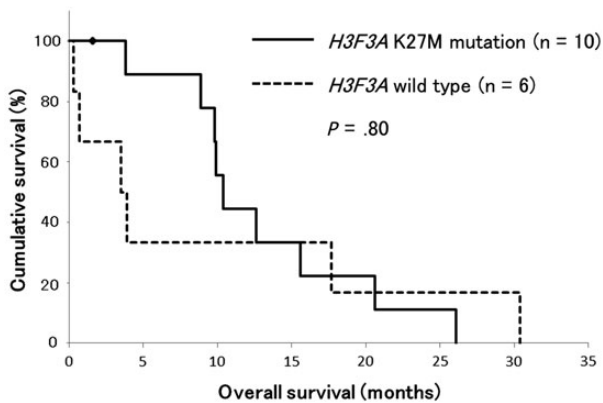


Fig. 3. Kaplan-Meier estimates of overall survival in cases of high-grade thalamic gliomas. There was no statistical difference in overall survival between patients with *H3F3A* K27M-mutant tumors and those with wild-type *H3F3A* tumors.

The Cox regression analysis assessing 3 variables—*H3F3A* K27M mutation status, *MGMT* methylation, and age—showed no significant difference in overall survival due to any one variable (*H3F3A* mutation: hazard ratio [HR] = 0.11, 95% confidence interval [CI] = 0.0057–2.2, $P = .15$; *MGMT* methylation: HR = 0.088, 95% CI = 0.0054–1.4, $P = .088$; and age: HR = 0.96, 95% CI = 0.88–1.1, $P = .38$).

Discussion

Here, we showed that the *H3F3A* K27M mutation was common in high-grade thalamic gliomas in young adults, as is the case for GBM in children and adolescents.¹⁷ Reportedly, 80% of pediatric thalamic GBM tumors harbor the *H3F3A* K27M substitution,^{5,7,17} as do 71%–78% of DIPGs;^{6,8} however, the occurrence of this substitution in adult thalamic glioma has not been examined. We found that the *H3F3A* K27M mutation was highly prevalent in cases of thalamic GBM in young adults; moreover, this mutation was found in 90% (9/10 cases) of high-grade thalamic gliomas in patients between 20 and 46 years of age. In contrast to *IDH* mutations, the *H3F3A* K27M mutation seemed infrequent in low-grade gliomas; DAs from patients of 29 or 30 years of age did not have the *H3F3A* K27M mutation. For DIPGs, a small number of low-grade astrocytomas were reported to have the *H3F3A* K27M mutation,⁸ but in general the *H3F3A* K27M mutation seemed to be specific to high-grade gliomas.^{5,7,18}

H3F3A encodes H3.3, a specialized histone variant. H3.3 is deposited on chromatin in a replication-independent manner and is enriched at actively transcribed genes and heterochromatic regions, such as telomeres and pericentromeric regions.¹⁹ Histone 3 lysine 27 trimethylation (H3K27me3), which is mediated by the histone-methyltransferase enhancer of zeste homolog 2 (EZH2), a member of the Polycomb family, is associated with the silencing of transcription.²⁰ Reportedly, tumors with the *H3F3A* K27M

mutation have little or no H3K27me3, and they have increased acetylation of H3K27 (H3K27ac); conversely, tumors with wild-type *H3F3A* have increased H3K27me3 and lowered H3K27ac levels.^{21,22} Although the mutated histone variant H3.3 accounts for only a small proportion of the entire histone H3 population, reduction of H3K27me3 occurs globally and affects other histone H3 molecules because the K27M peptide reduces the methyltransferase activity of Polycomb repressive complex 2 (PRC2) by inhibiting the catalytic subunit EZH2, which contains a Su(var)3-9/enhancer-of-zeste/trithorax (SET) domain.²² Moreover, inhibition of PRC2 leads to increased levels of H3K27 acetylation, which is a marker of active enhancers.²³ In fact, gliomas with the *H3F3A* K27M mutation were shown to form a class with a distinctive methylation profile of CpG islands that probably resulted from epigenetic dysregulation.⁷ However, the mechanisms by which this dysregulation of histone modification leads to gliomagenesis is unknown. We reasoned that the thalamic gliomas lacking the *H3F3A* mutation might result from a similar mechanism of tumorigenesis as tumors harboring the *H3F3A* K27M mutation; therefore, we performed targeted gene sequencing of molecules that could modulate H3K27 status. The targeted genes included *EZH2*, *KDM6A*, *EP300*, and *CREBBP*. We identified a *KDM6A* mutation (p.R1213L) in one case of DA. This mutation was located in the JmjC domain, and might have similar tumorigenic potential as the *H3F3A* K27M mutation. We also identified a *CREBBP* mutation in a tumor with the *H3F3A* K27M mutation; however, we did not find mutations in any of these genes in the high-grade tumors that lacked the *H3F3A* K27M mutation. Therefore, high-grade thalamic gliomas with wild-type *H3F3A* might have resulted from a tumorigenic mechanism that is not related to H3.3 K27 modifications. However, we did not identify any other driver mutation. Genomic analysis on a larger scale might be required to reveal novel mutations, but thalamic gliomas are rare and biopsy is the standard surgical procedure; therefore, such a large-scale analysis of these gliomas will be difficult.

To further evaluate the molecular characteristics of *H3F3A* K27M-mutant thalamic gliomas, global methylation profiles were examined; the adult thalamic high-grade gliomas with the *H3F3A* K27M mutation had methylation profiles similar to those of *H3F3A* K27M-mutant pediatric glioblastomas. This finding indicated that patient age did not affect the pattern of methylation in K27M-mutant tumors. In contrast, *H3F3A* wild-type adult thalamic high-grade gliomas, which occurred mostly in patients over 50 years of age, shared the molecular characteristics with hemispheric glioblastomas; this finding was expected based on the fact that molecules that could modulate H3K27 status were not mutant in these tumors. These results raised the possibility that treatment strategies in cases of adult glioblastomas should be designed based on tumor location and *H3F3A* mutation status.

In this set of cases, the median overall survivals were only 8.9 months and 15.6 months for patients with GBM and those with AA, respectively. These periods of survival were shorter than the average overall survival among patients with GBM or AA.²⁴ These gliomas, because of their location, were not amenable to radical tumor resection, and this characteristic might be one reason for the poor outcomes, as the degree of surgical resection is an important prognostic factor.²⁵ Indeed, diagnostic biopsy was the sole surgical intervention in most of these cases. The absence of *IDH1* and *IDH2* mutations, which were found in ~30% of AA and 10% of GBM in our previous report¹⁶ and are good prognostic markers of longer

survival, might also account for the poor prognosis of patients with thalamic gliomas. We also suspected that the low frequency of methylated *MGMT* promoters, which are the key indicators of poor response to temozolomide and are among the most important prognostic factors,²⁶ might explain the poor survival among younger patients with thalamic glioma who underwent intensive chemoradiotherapy. Indeed, the patients with methylated *MGMT* promoters lived longer than those with unmethylated *MGMT* promoters, but this difference was not statistically significant. In addition, we suspected that *H3F3A* K27M mutation in thalamic gliomas might be associated with poor survival, because *H3F3A* K27M-mutant DIPGs were reportedly associated with worse overall survival than were wild-type tumors.⁸ However, in this study, there was no significant difference in overall survival between patients with *H3F3A* K27M-mutant gliomas, which occurred mostly in younger patients, and those with wild-type *H3F3A* gliomas, which occurred mostly in older patients. Nevertheless, our sample size was small, and the prognostic significance of *H3F3A* K27M mutation for thalamic gliomas must be examined further in larger studies.

In conclusion, thalamic gliomas in young adults, as well as those in children and adolescents, often harbor the *H3F3A* K27M mutation. Thalamic high-grade gliomas in young adults may as a group share a particular mechanism of tumorigenesis that is related to the *H3F3A* K27M mutation; therefore, development of customized treatment strategies may be required for this patient population.

Supplementary Material

Supplementary material is available online at Neuro-Oncology (<http://neuro-oncology.oxfordjournals.org/>).

Funding

This work was supported in part by the National Cancer Center Research and Development Fund (23-A-20), and by Grants-in-Aid for Scientific Research (B) (no. 23390343 to A.M.), Grant-in-Aid for Scientific Research (S) (no. 24221011 to H.A.), Grant-in-Aid for Scientific Research on Innovative Areas (no. 23134501 to A.M.), Grant-in-Aid for Young Scientists (B) (no. 24791486 to K.S.), and a research program of the Project for Development of Innovative Research on Cancer Therapeutics (P-Direct) (A.M., G.N., Y.N., H.A., N.S.) from the Ministry of Education, Culture, Sports, Science, and Technology of Japan. A.M. was also supported by the Takeda Science Foundation and Japan Brain Foundation.

Acknowledgments

The authors thank Reiko Matsuura and Yuko Matsushita for extracting DNA from formalin-fixed, paraffin-embedded samples and blood, Hiroko Meguro for performing the Infinium methylation assays, Kaori Shiina and Saori Kawanabe for gene sequencing, and Ruriko Miyahara for assisting with the analysis of patient information.

Conflict of interest statement. None declared.

References

- Cheek WR, Taveras JM. Thalamic tumors. *J Neurosurg.* 1966;24(2): 505–513.

2. McKissock W, Paine KW. Primary tumours of the thalamus. *Brain*. 1958; 81(1):41–63.
3. Tovi D, Schisano G, Liljeqvist B. Primary tumors of the region of the thalamus. *J Neurosurg*. 1961;18:730–740.
4. Kelly PJ. Stereotactic biopsy and resection of thalamic astrocytomas. *Neurosurgery*. 1989;25(2):185–194.
5. Schwartzentruber J, Korshunov A, Liu XY, et al. Driver mutations in histone H3.3 and chromatin remodelling genes in paediatric glioblastoma. *Nature*. 2012;482(7384):226–231.
6. Wu G, Broniscer A, McEachron TA, et al. Somatic histone H3 alterations in pediatric diffuse intrinsic pontine gliomas and non-brainstem glioblastomas. *Nat Genet*. 2012;44(3):251–253.
7. Sturm D, Witt H, Hovestadt V, et al. Hotspot mutations in *H3F3A* and *IDH1* define distinct epigenetic and biological subgroups of glioblastoma. *Cancer Cell*. 2012;22(4):425–437.
8. Khuong-Quang DA, Buczkowicz P, Rakopoulos P, et al. K27M mutation in histone H3.3 defines clinically and biologically distinct subgroups of pediatric diffuse intrinsic pontine gliomas. *Acta Neuropathol*. 2012; 124(3):439–447.
9. Li H, Durbin R. Fast and accurate short read alignment with Burrows–Wheeler transform. *Bioinformatics*. 2009;25(14):1754–1760.
10. McKenna A, Hanna M, Banks E, et al. The Genome Analysis Toolkit: a MapReduce framework for analyzing next-generation DNA sequencing data. *Genome Res*. 2010;20(9):1297–1303.
11. Wang K, Li M, Hakonarson H. ANNOVAR: functional annotation of genetic variants from high-throughput sequencing data. *Nucleic Acids Res*. 2010;38(16):e164.
12. Robinson JT, Thorvaldsdottir H, Winckler W, et al. Integrative genomics viewer. *Nat Biotechnol*. 2011;29(1):24–26.
13. Esteller M, Sanchez-Cespedes M, Rosell R, Sidransky D, Baylin SB, Herman JG. Detection of aberrant promoter hypermethylation of tumor suppressor genes in serum DNA from non-small cell lung cancer patients. *Cancer Res*. 1999;59(1):67–70.
14. Cancer Genome Atlas Research Network. Comprehensive genomic characterization defines human glioblastoma genes and core pathways. *Nature*. 2008;455(7216):1061–1068.
15. Fontebasso AM, Schwartzentruber J, Khuong-Quang DA, et al. Mutations in *SETD2* and genes affecting histone H3K36 methylation target hemispheric high-grade gliomas. *Acta Neuropathol*. 2013; 125(5):659–669.
16. Mukasa A, Takayanagi S, Saito K, et al. Significance of *IDH* mutations varies with tumor histology, grade, and genetics in Japanese glioma patients. *Cancer Sci*. 2012;103(3):587–592.
17. Fontebasso AM, Liu XY, Sturm D, Jabado N. Chromatin remodeling defects in pediatric and young adult glioblastoma: a tale of a variant histone 3 tail. *Brain Pathol*. 2013;23(2):210–216.
18. Gielen GH, Gessi M, Hammes J, Kramm CM, Waha A, Pietsch T. *H3F3A* K27M mutation in pediatric CNS tumors: a marker for diffuse high-grade astrocytomas. *Am J Clin Pathol*. 2013;139(3):345–349.
19. Goldberg AD, Banaszynski LA, Noh KM, et al. Distinct factors control histone variant H3.3 localization at specific genomic regions. *Cell*. 2010;140(5):678–691.
20. Vastenhouw NL, Schier AF. Bivalent histone modifications in early embryogenesis. *Curr Opin Cell Biol*. 2012;24(3):374–386.
21. Venneti S, Garimella MT, Sullivan LM, et al. Evaluation of histone 3 lysine 27 trimethylation (H3K27me3) and enhancer of zest 2 (EZH2) in pediatric glial and glioneuronal tumors shows decreased H3K27me3 in *H3F3A* K27M mutant glioblastomas. *Brain Pathol*. 2013;23(5): 558–564.
22. Lewis PW, Muller MM, Koletsky MS, et al. Inhibition of PRC2 activity by a gain-of-function H3 mutation found in pediatric glioblastoma. *Science*. 2013;340(6134):857–861.
23. Zhou VW, Goren A, Bernstein BE. Charting histone modifications and the functional organization of mammalian genomes. *Nat Rev Genet*. 2011;12(1):7–18.
24. Shibui S. Report of Brian Tumor Registry of Japan (1984–2000). *Neural Med Chir (Tokyo)*. 2009;49:1–101.
25. Sanai N, Polley MY, McDermott MW, Parsa AT, Berger MS. An extent of resection threshold for newly diagnosed glioblastomas. *J Neurosurg*. 2011;115(1):3–8.
26. Hegi ME, Diserens AC, Gorlia T, et al. *MGMT* gene silencing and benefit from temozolomide in glioblastoma. *N Engl J Med*. 2005;352(10): 997–1003.